



Design, synthesis, and biological evaluation of 3-(1-benzotriazole)-nor- β -lapachones as NQO1-directed antitumor agents

Li-Qiang Wu^{a,b}, Xin Ma^a, Zhao-Peng Liu^{b,*}

^a School of Pharmacy, Xinxiang Medical University, Xinxiang 453003, PR China

^b Department of Medicinal Chemistry, Key Laboratory of Chemical Biology (Ministry of Education), School of Pharmaceutical Sciences, Cheeloo College of Medicine, Shandong University, Jinan 250012, PR China

ARTICLE INFO

Keywords:

nor- β -Lapachone
Benzotriazole
NQO1-directed antitumor agents
Antitumor

ABSTRACT

A series of novel 3-(1-benzotriazole)-nor- β -lapachones **5a–5l** were synthesized as the NQO1-targeted anticancer agents. Most of these compounds displayed good antiproliferative activity against the breast cancer MCF-7, lung cancer A549 and hepatocellular carcinoma HepG2 cells in agreements with their NQO1 activity. Among them, compound **5k** was identified as a favorable NQO1 substrate. It could activate the ROS production in a NQO1-dependent manner, arrest tumor cell cycle at G0/G1 phase, promote tumor cell apoptosis, and decrease the mitochondrial membrane potential. In HepG2 xenograft models, **5k** significantly suppressed the tumor growth with no influences on animal body weights. Therefore, **5k** could be a good lead for further anticancer drug developments.

1. Introduction

Cancer ranks the second primary cause of death and more than 18 million new cancer patients and 9 million cancer-related deaths are reported each year worldwide [1]. Chemotherapy is one of the most effective strategies for cancer treatment. Nonetheless, a majority of antitumor drugs used in clinic have toxicity to the adjacent non-carcinoma tissues and a variety of side reactions, thus limiting the therapeutic effects. With the deep understanding of the molecular biology of cancer, molecular targeted drugs, including those that target the tumor occurrence and progression mechanisms, as well as the targeted delivery of precursors with or without toxicity to cancer tissues, become the major concerns in anticancer developments [2–5].

NAD(P)-H:quinone oxidoreductase-1 (NQO1, DT-diaphorase, EC1.6.99.2) is identified as one of the flavoenzymes catalyzing direct two-electron reduction for various quinones, with NADH or NADPH being served as the cofactor [6]. Due to the overexpression in certain tumor tissues, NQO1 is a potential target for anticancer drug discovery [7–10]. Both the natural and synthetic heterocyclic quinones, such as mitomycin (MMC), 2,5-diaziridinyl-3-(hydroxymethyl)-6-methyl-1,4-benzoquinone (RH1), streptonigrin (STN), lavendamycin, β -lapachone, tanshinone IIA, dunnione, deoxyxyboquinone (DNQ) and isobutyl-deoxyxyboquinone (IB-DNQ), have been proved to be cytotoxic to

cancer cells after bioreduction by NQO1 [9,11].

Lapachones exist in a variety of plant families, which have been utilized in the field of medicinal chemistry to synthesize derivatives that possess possible anti-tumor or anti-parasitic effects [12–19]. Nor- β -lapachone (nor- β -lap), an inferior homologue of β -lapachone (β -lap), exhibits potent antiproliferative activity a diverse of tumor cells with low cytotoxicity towards normal cells [20,21]. Based on the nor- β -lap prototype, a number of nor- β -lap derivatives, including 3-arylamino and 3-alkoxy-nor- β -lapachones [14], 3-phenylthio-nor- β -lapachone [22], nor- β -lapachone-based chalcones [23], and 1,2,3-triazole-nor- β -laps [24–25], were synthesized and evaluated as antitumor agents. The antitumor effects of nor- β -lap is associated with the reactive oxygen species (ROS) production and tumor cell destruction with increased endogenous NQO1 contents [26] (Fig. 1).

Molecular docking study between nor- β -lap and NQO1 shows that nor- β -lap generates potent π - π stacking with FAD (a coenzyme) isopyrazine, which is efficiently embedded into the NQO1 active pocket (Fig. 2). However, one side pocket (II) generated by Met131, Met154, Phe236, Tyr128 and His161 residues was not occupied by nor- β -lap. In previous studies, Cardoso *et al.* discovered that 3-(4-phenyl-1,2,3-triazol)-nor- β -lap displayed much more promising therapeutic index relative to the classical therapeutic agents [27]. To find more potent antitumor agents, in this study, we merged the benzene ring and the

* Corresponding author.

E-mail address: liuzhaop@sdu.edu.cn (Z.-P. Liu).

<https://doi.org/10.1016/j.bioorg.2021.104995>

Received 12 October 2020; Received in revised form 7 May 2021; Accepted 14 May 2021

Available online 19 May 2021

0045-2068/© 2021 Elsevier Inc. All rights reserved.

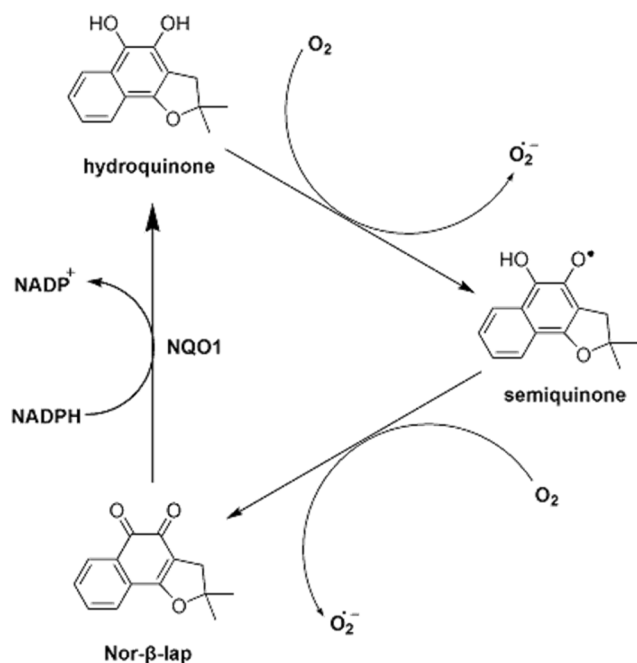


Fig. 1. The action mechanism of nor- β -lap.

1,2,3-triazol moiety in 3-(4-phenyl-1,2,3-triazol)-nor- β -lap into the benzotriazole scaffold in the design of novel NQO1-directed antitumor agents, considering the benzotriazole scaffold is widely used in the design of anticancer agents for a multiple of tumor targets [28]. In the designed 3-(1-benzotriazole)-nor- β -lapachones **5a–5l**, a benzotriazole moiety at the 3-position of nor- β -lap is expected to interact with the side pocket that is not occupied by nor- β -lap so as to increase the interaction with NQO1 and thus enhance their anticancer effects (Fig. 2).

2. Results and discussion

2.1. Chemistry

Scheme 1 presents the synthetic route for compounds **5a–5l**. First, the tetralones **1** autoxidation in the presence of potassium *tert*-butoxide and oxygen produced the lawsones **2**, which was then converted to nor-lapachol **3** via a Michael addition reaction with methylamine and isobutyraldehyde, followed by an elimination reaction induced by *p*-toluenesulfonic acid (*p*-TsOH). Finally, the cyclization of nor-lapachol **3** in the presence of bromine generates the 3-bromo-nor- β -lapachone intermediate **4** that was reacted with benzotriazoles to generate the 3-(1-benzotriazole)-nor- β -lapachones **5a–5l**. The structures of these novel compounds were confirmed by the HRMS, ^1H NMR, ^{13}C NMR and IR

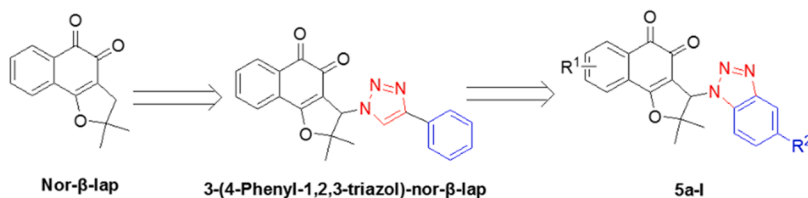


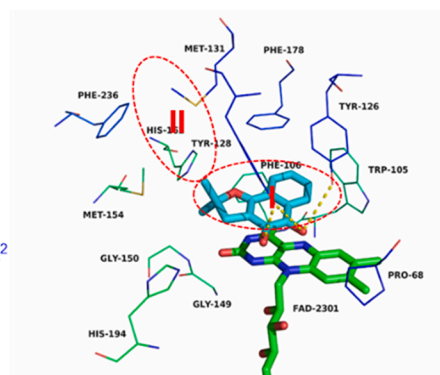
Fig. 2. Design of novel 3-(1-benzotriazole)-nor- β -lapachones.

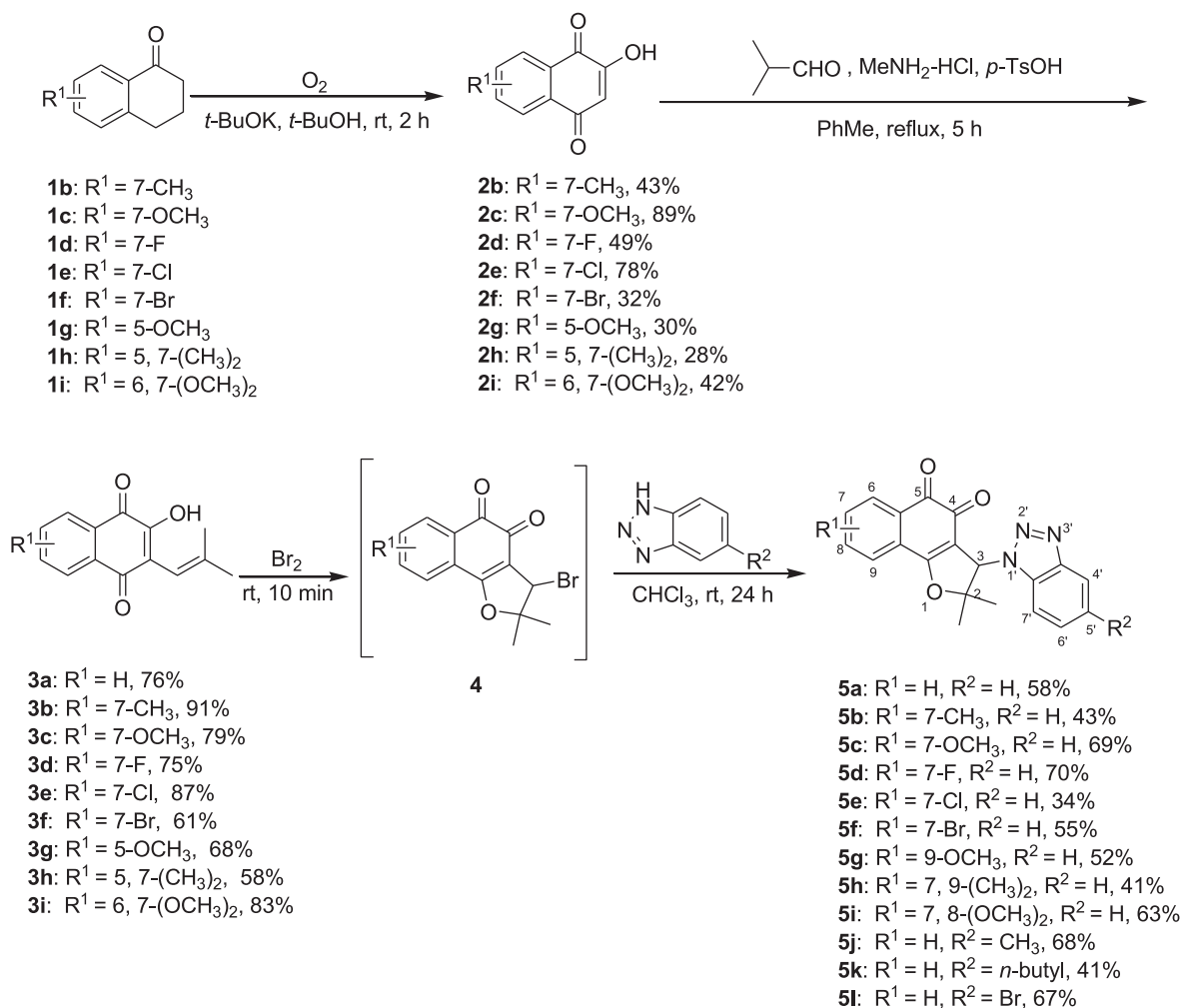
analysis. For example, the HRMS of **5i** showed one $[\text{M} + \text{Na}]^+$ quasi-molecular ion peak at $m/z = 428.1214$, indicating its molecular formula of $\text{C}_{22}\text{H}_{19}\text{N}_3\text{O}_5$. In the ^1H NMR spectra of **5i**, five peak pairs were observed at 7.25, 7.34–7.36, 7.42, 7.65 and 8.06 ppm, separately, which characterized the presence of seven aromatic hydrogens. In addition, three singlets were also observed at 1.11, 1.81, 4.02, 4.08 and 6.28 ppm, which were attributed to two CH_3 protons, two OCH_3 protons and one CH proton of the 3-substituted tetrahydrofuran, respectively. In the ^{13}C NMR spectra of **5i**, 22 different resonances were observed, including five typical signals detected at $\delta = 65.8$ ppm (due to the C-3 group), 174.9 and 179.3 ppm (two carbonyls), 21.3 and 28.0 ppm (two nonequivalent CH_3 groups). Besides, $\text{C}=\text{O}$ absorptions (1653 and 1612 cm^{-1}) were observed from the IR spectrum for **5i**. In addition, the ^1H and ^{13}C NMR spectra of the compound was fully assigned by HMBC, DEPT135 and HSQC (see experiments and supplementary data).

The 3-(4-aryl-1,2,3-triazol)-nor- β -laps **8a** and **8b** were reported to be antitumor agents [27]. For a direct comparison, we prepared them and a new derivative **8c** according to the literature method [24]. The Huisgen 1,3-dipolar cycloaddition reaction between 3-azido-2,2-dimethyl-2,3-dihydro-naphtho[1,2-*b*]furan-4,5-dione **6** and the appropriate terminal alkynes **7** catalyzed by Cu(I) generated the only 1,4-regioisomers (Scheme 2).

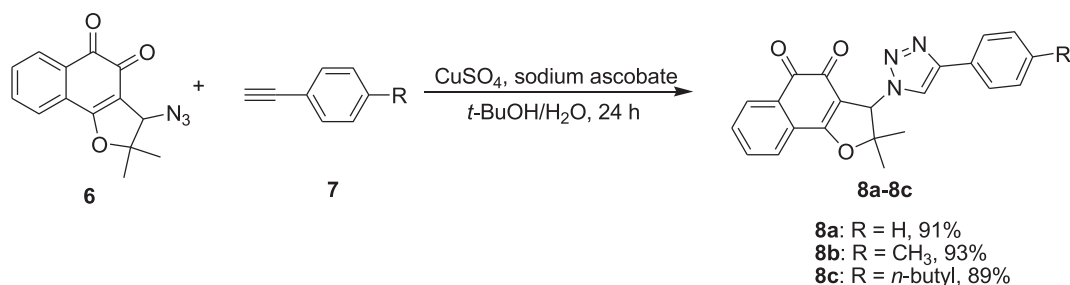
2.2. Measurement of the NQO1-induced **5** and **8** metabolic rates

The 3-(1-benzotriazole)-nor- β -lapachones **5a–5l** and 3-(4-aryl-1,2,3-triazol)-nor- β -laps **8a–8c** were assessed at the concentration of 10 mmol/L to determine whether they might serve as the substrates for NQO1. They were co-incubated with NADPH as well as human NQO1, respectively, and the absorbance value of NADPH was measured at 340 nm by a microplate reader. The metabolic rates of **5a–5l** and **8a–8c** by NQO1 were presented as $\mu\text{mol NADPH}/\text{min}/\mu\text{mol NQO1}$. A relatively larger number of NADPH are oxidized to NADP^+ if the compound is a better NQO1 substrates. As shown in Table 1, all these 3-(1-benzotriazole)-nor- β -lapachone derivatives except compound **5k** had lower metabolic rates than the positive control nor- β -lap ($682\ \mu\text{mol}$ oxidized NADPH/ $\mu\text{mol NQO1}/\text{minute}$). The R^1 group at the *ortho*-naphthoquinone and the R^2 group at benzotriazole greatly affected NQO1 activity. Compound **5a** with no substitution at the *ortho*-naphthoquinone and benzotriazole had a relatively good medium NQO1-induced metabolic rate. The substituents *ortho*-naphthoquinone showed quite different influences on the metabolic rates. A 7-methyl (**5b**) or 7-bromo (**5f**) at the nor- β -lap core was well tolerated, a 7-methoxy (**5c**) was moderately tolerated, but the 7-F (**5d**) or 7-Cl (**5e**) greatly reduced the activity. Moreover, the substitution at the 9-position by methoxy group (**5g**) and the disubstitution at the 7,8- (**5h**) and 7,9-positions (**5i**) were not tolerated. For the substituents at the benzotriazole 5-position, the methyl (**5j**) or Br (**5l**) greatly reduced the activity, while a *n*-butyl group (**5k**) increased the metabolic rate,





Scheme 1. Synthesis of 3-(1-benzotriazole)-nor-β-lapachones.



Scheme 2. Synthesis of 3-(4-aryl-1,2,3-triazol)-nor-β-laps.

indicating that **5k** was a good or better as substrate for NQO1 as that of nor-β-lap. For 3-(4-aryl-1,2,3-triazol)-nor-β-laps, as shown in Table 2, they had lower metabolic rates than the positive control nor-β-lap and the corresponding 3-(1-benzotriazole)-nor-β-lapachones. The overall structure–activity relationships (SARs) of synthesized compounds were summarized in Fig. 3.

2.3. Molecular modeling

Molecular docking simulations were carried out based on the NQO1 (PDB ID: 2F10) crystal structure to predict the possible binding mode of **5k** and **8c** with NQO1. As shown in Fig. 4A, compounds **5k** formed the π-stacking with the FAD isoalloxazine ring, and its two carbonyls

interacted with Tyr126 and Tyr128 through hydrogen bonds. In addition, the 5-butyl-1-benzotriazole moiety extended the side II pocket and formed π-stacking with Tyr128 at NQO1 active site that may account for it as a favorable substrate for NQO1. Compound **5k** had a higher activity in comparison with **8c**, which was probably attributed to its benzotriazole group that served as a more appropriate moiety to stabilize the π-stacking interactions with the key amino acid residues such as Tyr128 in the catalytic site of NQO1 (Fig. 4).

2.4. Antiproliferative activity in vitro

The 3-(1-benzotriazole)-nor-β-lapachone derivatives that showed relatively lower (**5g**), medium (**5a**, **5b**, **5f**) and higher (**5k**) NQO1

Table 1
The results for 5a–5k NQO1 activities.

| Compound | R ¹ | R ² | NQO1 activity ^a |
|------------------|--------------------------------------|-----------------|----------------------------|
| 5a | H | H | 586 ± 17 |
| 5b | 7-CH ₃ | H | 528 ± 34 |
| 5c | 7-OCH ₃ | H | 340 ± 13 |
| 5d | 7-F | H | 138 ± 10 |
| 5e | 7-Cl | H | 168 ± 5 |
| 5f | 7-Br | H | 541 ± 17 |
| 5g | 9-OCH ₃ | H | 80 ± 13 |
| 5h | 7,9-(CH ₃) ₂ | H | 142 ± 15 |
| 5i | 7,8-(OCH ₃) ₂ | H | 99 ± 21 |
| 5j | H | CH ₃ | 288 ± 29 |
| 5k | H | <i>n</i> -butyl | 735 ± 13 |
| 5l | H | Br | 266 ± 30 |
| nor-β-lap | | | 682 ± 24 |

^a μmol NADPH/μmol NQO1/min.

Table 2
The results for 8a–8c NQO1 activities.

| Compound | R | NQO1 activity ^a |
|------------------|-------------------|----------------------------|
| 8a | H | 234 ± 19 |
| 8b | 4-CH ₃ | 131 ± 23 |
| 8c | <i>n</i> -butyl | 326 ± 26 |
| nor-β-lap | | 682 ± 35 |

^a μmol NADPH/μmol NQO1/min.

activities and 3-(4-aryl-1,2,3-triazol)-nor-β-lap derivative **8c** were assayed for their antiproliferative effects against the NQO1 abundant breast cancer MCF-7, lung cancer A549 and hepatocellular carcinoma HepG2 cells by traditional 3-(4,5-Dimethylthiazol-2-yl)-2,5-diphenyltetrazolium bromide (MTT) method, using nor-β-lap as the positive reference. The results were shown in Table 3.

In general, these three tumor cells showed different sensitivity towards the 3-(1-benzotriazole)-nor-β-lapachones and 3-(4-aryl-1,2,3-triazol)-nor-β-lap. In agreement with its favorable activity as a NQO1 substrate, compound **5k** exhibited similar or more potent antiproliferative activities against the MCF-7, A549 and HepG2 cells. As the poor substrate for NQO1, compound **5g** was the least potent in comparison with nor-β-lap and the other four 3-(1-benzotriazole)-nor-β-lapachones against A549 and HepG2 cells, but was highly active against the MCF-7 cells. Among the compounds that had slightly lower NQO1 activity than nor-β-lap, **5f** was potent against all the three tumor

Table 3
The tumor cell growth inhibitory activity of the representative compounds.

| Comp. | IC ₅₀ (μM) | | |
|------------------|-----------------------|--------------|--------------|
| | MCF-7 | HepG2 | A549 |
| 5a | 2.14 ± 0.16 | 1.92 ± 0.16 | 10.70 ± 0.74 |
| 5b | 1.99 ± 0.25 | 1.74 ± 0.16 | 5.41 ± 0.59 |
| 5f | 1.75 ± 0.20 | 2.03 ± 0.03 | 2.06 ± 0.09 |
| 5g | 1.53 ± 0.10 | 13.79 ± 0.66 | 14.72 ± 0.52 |
| 5k | 2.64 ± 0.23 | 2.40 ± 0.44 | 0.49 ± 0.05 |
| 8c | 3.15 ± 0.96 | 2.96 ± 0.93 | 1.95 ± 0.23 |
| nor-β-lap | 13.07 ± 1.70 | 3.34 ± 0.31 | 11.71 ± 1.27 |

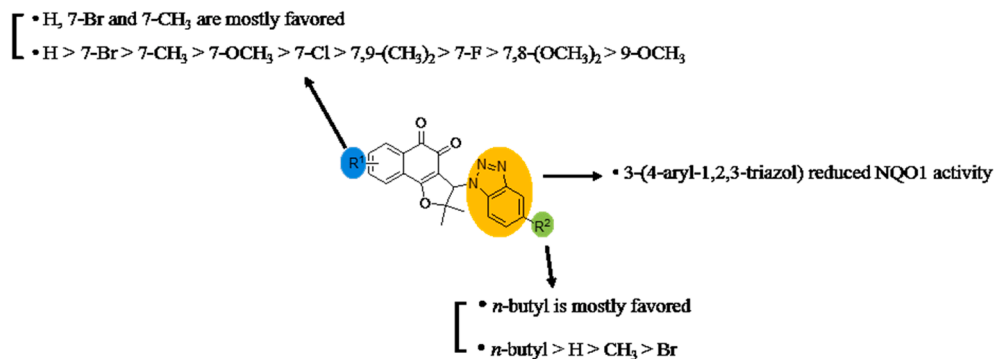


Fig. 3. Summarized SARs of target compounds.

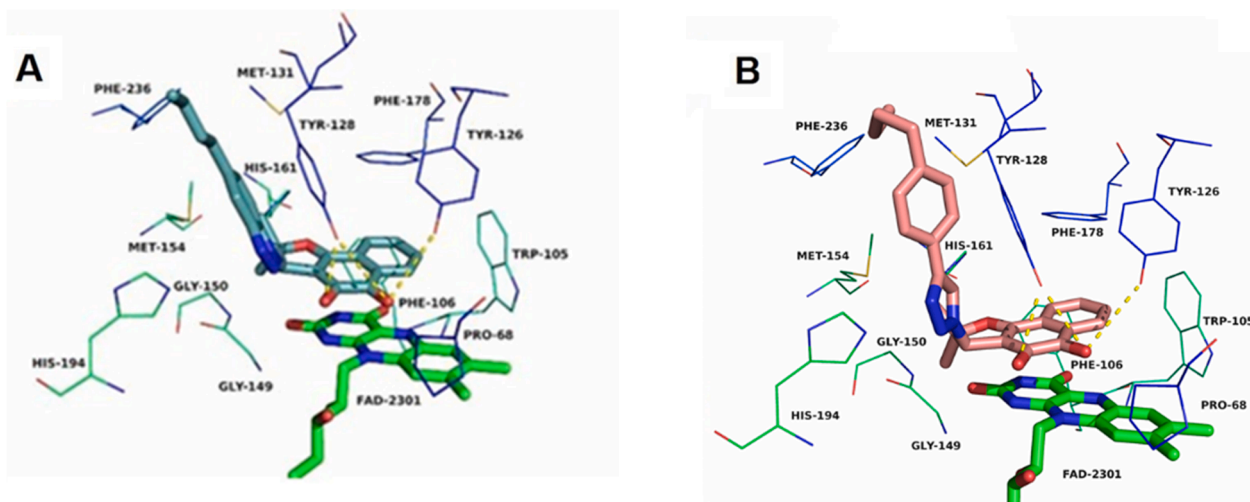


Fig.4. Molecular docking of compounds 5k (A) and 8c (B) with NQO1.

cell lines, while **5a** and **5b** exhibited higher antiproliferative activity against the MCF-7 and HepG2 cells, but were less active towards the A549 cells as that of nor- β -lap. Similar to its NQO1 activity, the 3-(4-aryl-1,2,3-triazol)-nor- β -lap derivative **8c** displayed lower antiproliferative activity against the three tumor cell lines than the corresponding 3-(1-benzotriazole)-nor- β -lapachone derivative **5k**. When judging in terms of the NQO1 activity as the NQO1 substrate as well as the balanced tumor growth inhibitory activity, **5k** was selected in the subsequent biological evaluations.

To further confirm the antiproliferative effects of **5k** is directly linked to its NQO1 interaction, **5k** was co-incubated with a NQO1 inhibitor, DIC [29], or a ROS scavenger, *N*-acetyl cysteine (NAC) [30], in A549 and HepG2 cells, and the results were summarized in Table 4. In the presence of DIC or NAC, the inhibitory effects of **5k** on HepG2 and A549 cells decreased by nearly 2-fold and 7-fold, respectively, supporting **5k** as the NQO1 substrate at the cellular levels. Moreover, **5k** was slightly less cytotoxic for the normal liver LO2 cells over the HepG2 cells.

2.5. Effects of **5k** on HepG2 cell cycles

To better understand the effects of **5k** on cell growth and division, flow cytometric analysis was conducted to assess cell cycle distribution of HepG2 cells exposed to **5k** for 24 h at the concentrations of 0.5, 1.0 and 2.0 μ M, respectively. As shown in Fig. 5, the control group had 46.76% HepG2 cells in the G0/G1 phase. Compound **5k** promoted HepG2 cell cycle arrest at the G0/G1 phase in a concentration dependent manner, with the G0/G1 cells of 49.51%, 52.39% and 56.75% at 0.5, 1.0 and 2.0 μ M, respectively.

2.6. Effects of **5k** on HepG2 cell apoptosis

Apoptosis, one of the spontaneous processes under the control of genes, exerts an important part in the homeostasis of tissues and in elimination of the unnecessary cells with no influence on the normal/unaffected cells. In this study, Annexin V and PI staining was utilized to determine the necrotic and apoptotic cell proportions through flow cytometric analysis. As shown in Fig. 6, there were 6.75% apoptotic HepG2 cells in the control group (without drug treatment). After 24 h of **5k** treatments at the concentrations of 1.2, 2.4, and 4.8 μ M, the apoptotic cells (early as well as late apoptosis) increased from 17.21, 34.55, and 60.14%, respectively. In the presence of the DIC, **5k** caused a weaker apoptosis rate (23.89%), further confirming that **5k** promoted HepG2 cell apoptosis through the NQO1 targeting.

2.7. Effects of **5k** on mitochondrial membrane potential (MMP)

Decreased MMP is an early event in apoptotic cells. To further evaluate the effects of **5k** on MMP in HepG2 cells, the cells were treated with 1.2, 2.4 and 4.8 μ M of **5k**, and the collapsed MMP was determined by fluorescence probe JC-1. As shown in Figs. 7, **5k** dose-dependently increased the mitochondrial membrane depolarization, with the rates of 8.60%, 11.63 and 18.71%, respectively, at 1.2, 2.4 and 4.8 μ M, in comparison with that of untreated cells (1.89%). Therefore, **5k** induced the HepG2 cells apoptosis possibly via the mitochondria-mediated pathway.

Table 4
Cell growth inhibitory activity of **5k**.

| Compd. | IC ₅₀ (μ M) | | | | |
|-----------|-----------------------------|-----------------|-----------------|-----------------|-----------------|
| | HepG2 + DIC | A549 + DIC | HepG2 + NAC | A549 + NAC | LO2 |
| 5k | 3.45 \pm 0.16 | 3.15 \pm 0.14 | 3.79 \pm 0.06 | 3.22 \pm 0.09 | 3.84 \pm 0.23 |

2.8. Effects of **5k** on reactive oxygen species (ROS) levels

The ROS production is very important to the antitumor effects of the NQO1-directed agents. Therefore, the effects of **5k** on ROS production in HepG2 cells were detected by 2',7'-dichlorofluorescein (DCF) staining [31], and the results were summarized in Fig. 8. At the concentration of 5 μ M, **5k** time-dependently and significantly increased the ROS levels relative to the control. **5k** also showed comparable ROS formation ability as that of β -lap. Besides, in the presence of DIC, the ROS generation induced by **5k** significantly decreased.

Electrochemistry is the standard method for studying redox reactions and this method can effectively demonstrate a compound's ability to generate ROS. Therefore, we further evaluated the electrochemical behavior of compound **5k**. As illustrated in Fig. 9A, Eredox value of **5k** (-1.01 V) is similar to that of that of β -lap (-1.09 V) and nor- β -lap (-1.04 V). Since the lipid peroxidation is used as an intracellular indicator of oxidative stress, we also carried out the thiobarbituric reactive species (TBARS) assay as one more evidence for the generation of ROS. As shown in Fig. 9B, **5k** significantly increased the accumulation of the lipid peroxidation product TBARS in a concentration-dependent manner. These findings suggested that the NQO1 bioactivation-mediated production of ROS accounted for a vital mediator for the inducing tumor cell apoptosis by **5k**.

2.9. Antitumor activity of **5k** in vivo

For evaluating **5k**'s anticancer activity in vivo, female nude mice were given subcutaneous inoculation of HepG2 cells via the right flank. After 2 weeks, visible tumor occurred in each mouse. Then, all mice were randomly divided into 3 groups, namely, the control (normal saline), the positive control (β -lap, 20 mg/kg), and **5k** (20 mg/kg) groups. Five nude mice in each group were administrated intravenously once every two days for 19 consecutive days. The body weight and tumor volume of each mouse were measured and recorded every day. The results were summarized in Fig. 10. The treatment with **5k** significantly suppressed the tumor growth (Fig. 10, A–C). The mean tumor size decreased by 2.1-fold and the mean tumor weight decreased by 52.3% in comparison with the vehicle group. Moreover, the treatment with **5k** had little influences on animal body weights, indicating the 20 mg/kg dose of **5k** was well tolerated.

3. Conclusions

In summary, a series of 3-(1-benzotriazole)-nor- β -lapachones have been designed, synthesized and evaluated as the anticancer agents targeting the NQO1. Among them, compound **5k** was demonstrated as a favorable NQO1 substrate. It effectively inhibited the tumor HepG2, MCF-7 and A549 cell proliferation, arrested the HepG2 cell in G0/G1 phase, induced the HepG2 cell apoptosis through the mitochondria pathway, and promoted the ROS generation. In the HepG2 xenograft mouse model, at the dose of 20 mg/kg, **5k** effectively suppressed the tumor growth with no influences on animal body weights. Therefore, **5k** may be a good lead for further development of the NQO1-directed anticancer agents.

4. Experiments

4.1. Chemistry

β -Lap was obtained from Topscience Co., Ltd (Purity > 99%). Other reagents or solvents were commercially available. The ¹H NMR and ¹³C NMR spectra were measured on a Bruker 400 spectrometers. HRMS were measured on a Bruker micrOTOF-QIII mass spectrometer. Melting points were performed by a XT-4 binocular microscope and were uncorrected.

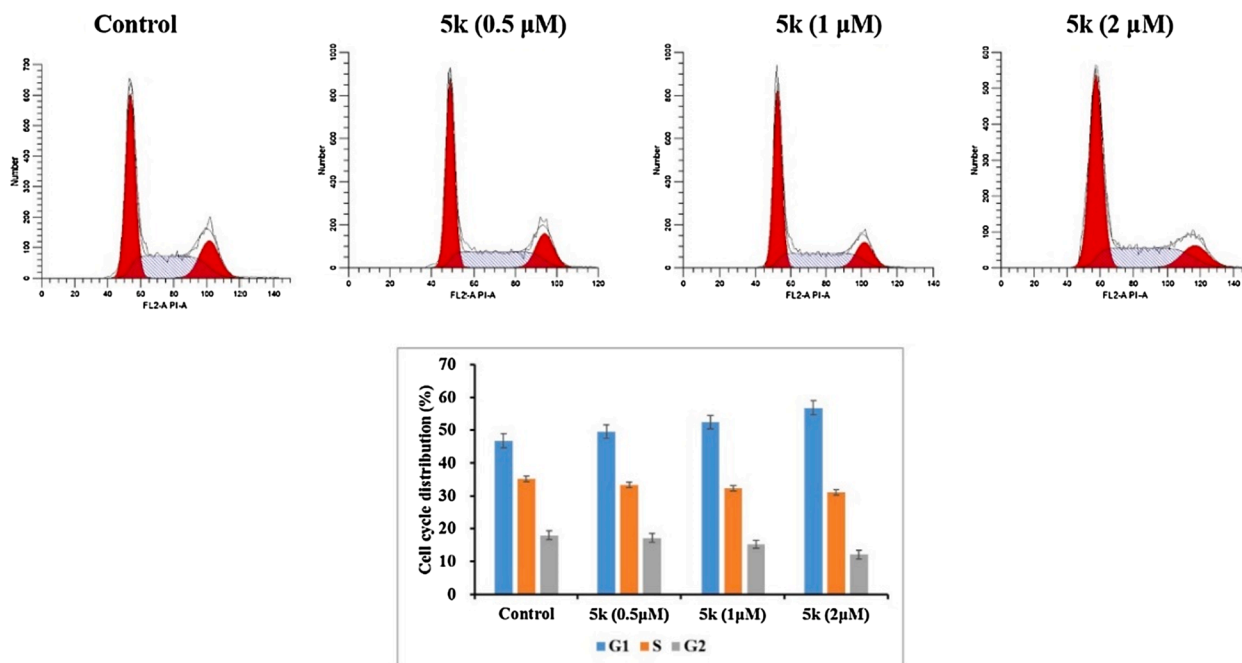


Fig. 5. Effects of 5k on HepG2 cell cycle.

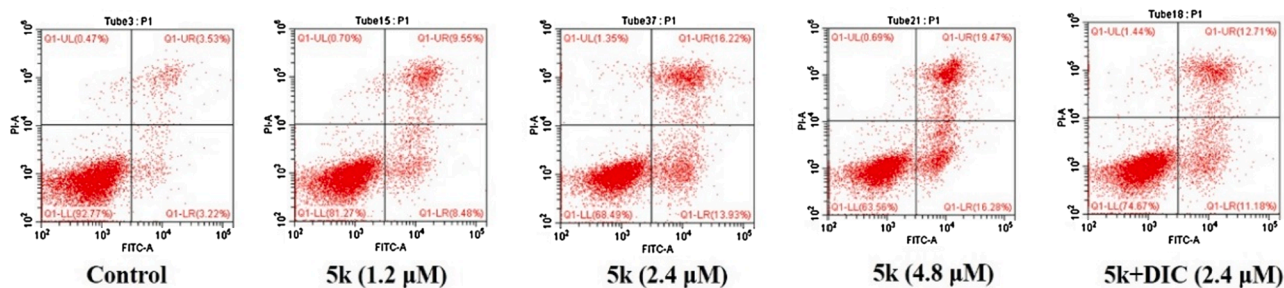


Fig. 6. Compound 5k induced HepG2 cell apoptosis.

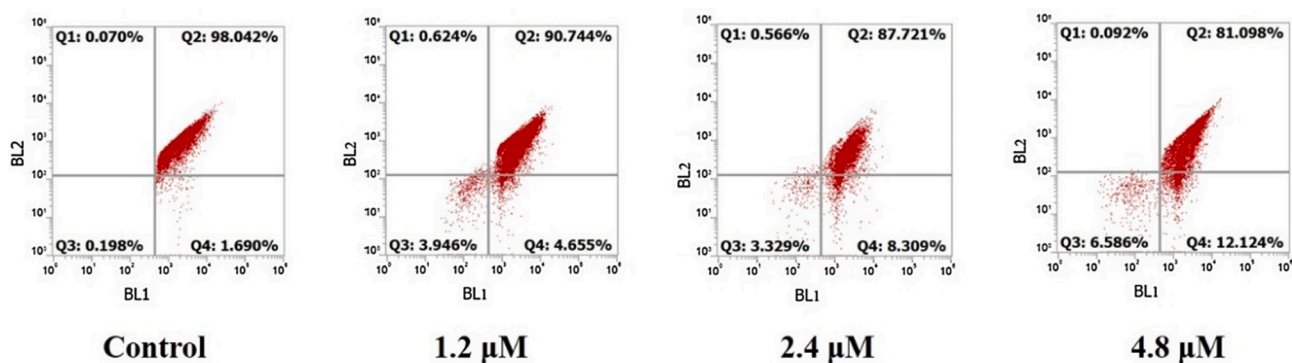


Fig. 7. Effects of 5k on MMP of HepG2 cells.

4.1.1. Synthesis of lawsone 2

Compound **2** was prepared according to literature method [32].

4.1.2. Synthesis of nor-lapachol 3

Nor-lapachol **3** was prepared according to literature method [33]. To a solution of lawsone **2** (10 mmol) in dry toluene (100 mL) was added methylamine hydrochloride (0.8 g, 12 mmol), isobutyraldehyde (4.6 mL, 50 mmol) and *p*-TsOH (2.28 g, 12 mmol). The reaction mixture was then refluxed in a system equipped with a Dean-Stark trap for 5 h. The

reaction mixture was then concentrated *in vacuo*, and the crude solid was purified by silica gel column chromatography using hexane/EtOAc as the eluent.

4.1.2.1. 2-Hydroxy-3-(2-methylprop-1-enyl)naphthalene-1,4-dione (3a)

Yellow solid, m.p. 110–111 °C (119–120 °C) [34], yield 76%; ¹H NMR (400 MHz, DMSO-*d*₆) δ: 10.95 (s, 1H), 8.01–7.95 (m, 2H), 7.85–7.79 (m, 2H), 5.84 (t, 1H, *J* = 1.2 Hz), 1.88 (d, 3H, *J* = 1.2 Hz), 1.55 (d, 3H, *J* = 0.8 Hz); ¹³C NMR (100 MHz, DMSO-*d*₆) δ: 184.7, 181.6, 154.5, 140.4,

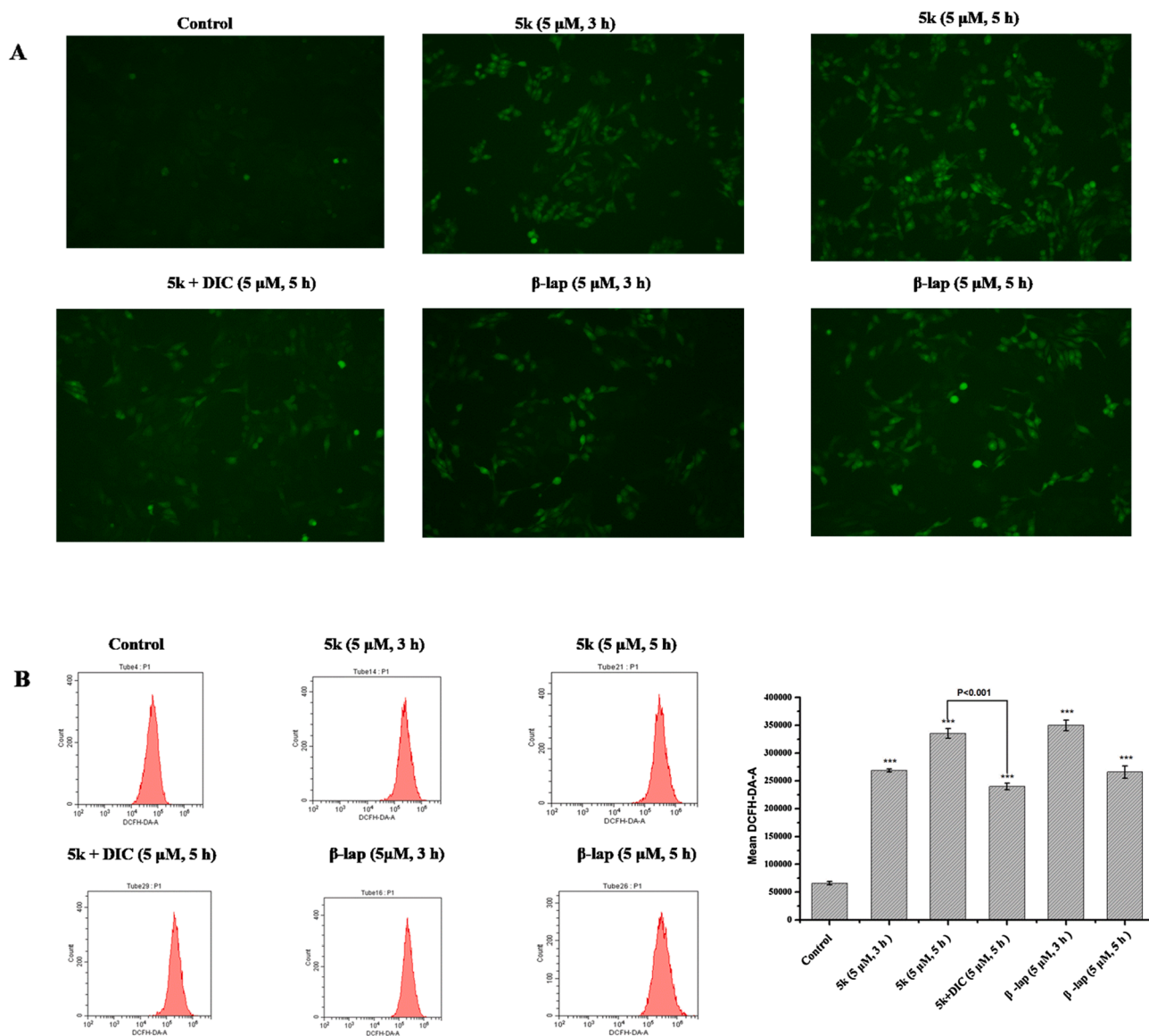


Fig. 8. Effects of 5k on ROS generation in HepG2 cells. A) ROS level by fluorescence microscopy; B) ROS level by flow cytometry analysis. *** $P < 0.001$ vs the control.

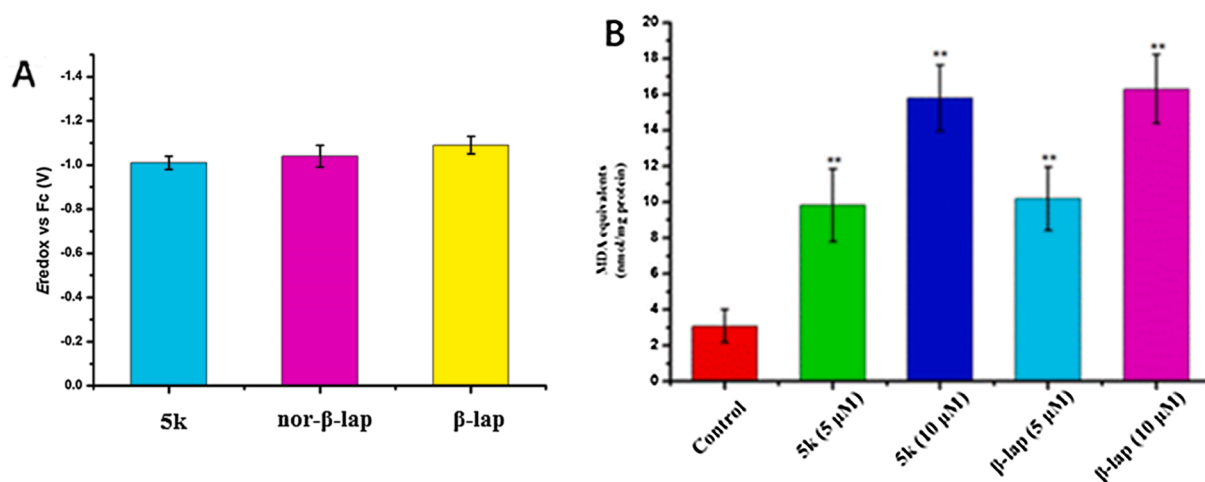


Fig. 9. A) Eredox of 5k vs Fc. Eredox values calculated as $(E_{pc} + E_{pa})/2$ are average values from voltammograms recorded at potential sweep rate of 50 mV/s; B) TBARS assay of 5k in HepG2 cells. Control (0.1% DMSO), ** $p < 0.01$ as compared to control.

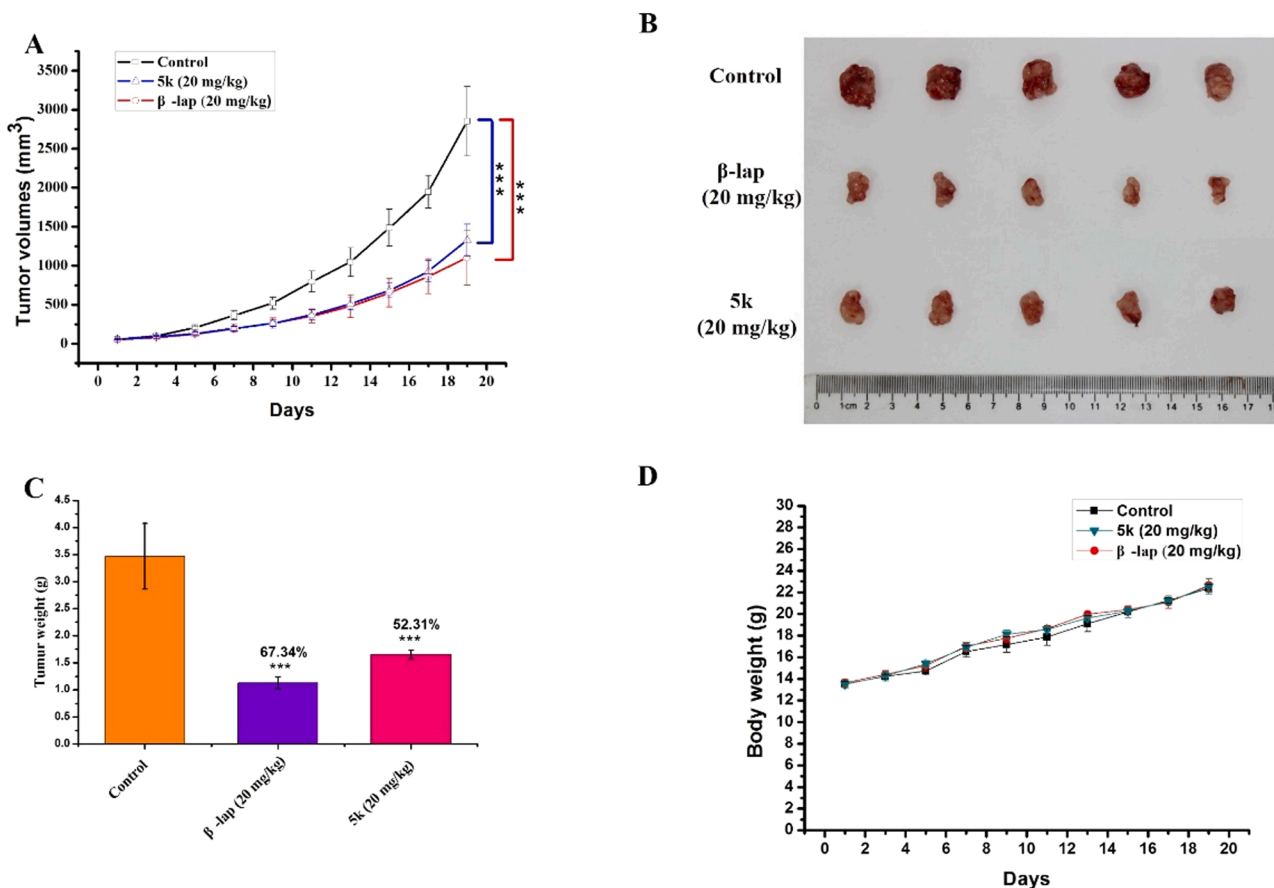


Fig. 10. Compound 5k inhibited the tumor growth in HepG2 xenograft nude mouse model. (A) Changes of tumor volume. (B) Images of the eventual tumor tissues. (C) Changes in tumor weights. (D) Changes in animal body weights. *** $P < 0.001$ compared with vehicle control.

135.0, 133.6, 132.6, 130.6, 126.3, 126.1, 121.0, 115.4, 26.5, 21.8; IR (KBr): 3358, 1642, 1590, 1452, 1375, 1300, 1270, 1070, 1043, 890, 794, 725, 669; HRMS-ESI (m/z): calcd for $C_{14}H_{12}NaO_3$ [$M + Na$]⁺ 251.0679, found: 251.0682.

4.1.2.2. 2-Hydroxy-7-methyl-3-(2-methylprop-1-enyl)naphthalene-1,4-dione (3b). Orange solid, m.p. 155–156 °C, yield 91%; ¹H NMR (400 MHz, DMSO- d_6) δ : 10.86 (s, 1H), 7.85–7.80 (m, 2H), 7.62 (dd, 1H, $J = 0.8, 7.6$ Hz), 5.83 (t, 1H, $J = 1.2$ Hz), 2.45 (s, 3H), 1.88 (d, 3H, $J = 1.2$ Hz), 1.54 (d, 3H, $J = 0.8$ Hz); ¹³C NMR (100 MHz, DMSO- d_6) δ : 184.6, 181.8, 154.3, 144.1, 140.3, 135.4, 130.5, 130.3, 126.4, 126.3, 120.8, 115.5, 26.5, 21.9, 21.5; IR (KBr): 3346, 1641, 1599, 1363, 1328, 1299, 1201, 1170, 1049, 915, 858, 824, 746, 670; HRMS-ESI (m/z): calcd for $C_{15}H_{14}NaO_3$ [$M + Na$]⁺ 265.0835, found: 265.0834.

4.1.2.3. 2-Hydroxy-7-methoxy-3-(2-methylprop-1-enyl)naphthalene-1,4-dione (3c). Orange solid, m.p. 156–157 °C, yield 79%; ¹H NMR (400 MHz, DMSO- d_6) δ : 10.80 (s, 1H), 7.89 (d, 1H, $J = 8.4$ Hz), 7.41 (d, 1H, $J = 2.8$ Hz), 7.32 (dd, 1H, $J = 2.8, 8.8$ Hz), 5.83 (t, 1H, $J = 1.2$ Hz), 3.92 (s, 3H), 1.88 (d, 3H, $J = 1.2$ Hz), 1.55 (d, 3H, $J = 1.2$ Hz); ¹³C NMR (100 MHz, DMSO- d_6) δ : 184.1, 181.5, 163.4, 154.1, 140.4, 132.4, 128.7, 125.8, 120.7, 120.5, 115.5, 110.1, 56.4, 26.5, 21.9; IR (KBr): 3381, 1658, 1632, 1591, 1448, 1380, 1300, 1228, 1198, 1041, 1015, 914, 856, 749, 508; HRMS-ESI (m/z): calcd for $C_{15}H_{14}NaO_4$ [$M + Na$]⁺ 281.0784, found: 281.0785.

4.1.2.4. 2-Hydroxy-7-fluoro-3-(2-methylprop-1-enyl)naphthalene-1,4-dione (3d). Orange solid, m.p. 140–141 °C, yield 68%; ¹H NMR (400 MHz, DMSO- d_6) δ : 11.04 (s, 1H), 8.02 (dd, 1H, $J = 1.2, 8.8$ Hz),

7.73–7.63 (m, 2H), 5.83 (t, 1H, $J = 1.2$ Hz), 1.89 (d, 3H, $J = 1.2$ Hz), 1.55 (d, 3H, $J = 0.8$ Hz); ¹³C NMR (100 MHz, DMSO- d_6) δ : 183.7, 180.6, 166.3 (d, $J_{C-F} = 252.9$ Hz), 154.7, 140.8, 133.2 (d, $J_{C-F} = 8.1$ Hz), 129.6 (d, $J_{C-F} = 9.1$ Hz), 129.3, 121.7 (d, $J_{C-F} = 22.3$ Hz), 121.0, 115.3, 112.5 (d, $J_{C-F} = 23.5$ Hz), 26.5, 21.9; IR (KBr): 3369, 2908, 1637, 1596, 1493, 1439, 1360, 1326, 1261, 1178, 1163, 1039, 922, 891, 856, 830, 748, 646; HRMS-ESI (m/z): calcd for $C_{14}H_{11}FNaO_3$ [$M + Na$]⁺ 269.0584, found: 269.0582.

4.1.2.5. 2-Hydroxy-7-chloro-3-(2-methylprop-1-enyl)naphthalene-1,4-dione (3e). Yellow solid, m.p. 146–147 °C, yield 78%; ¹H NMR (400 MHz, DMSO- d_6) δ : 11.10 (s, 1H), 7.96–7.93 (m, 2H), 7.87 (d, 1H, $J = 2.0$ Hz), 5.83 (t, 1H, $J = 1.2$ Hz), 1.88 (d, 3H, $J = 1.2$ Hz), 1.55 (d, 3H, $J = 0.8$ Hz); ¹³C NMR (100 MHz, DMSO- d_6) δ : 183.8, 180.6, 154.6, 140.9, 138.6, 134.5, 132.2, 131.1, 128.5, 125.5, 121.2, 115.2, 26.5, 21.9; IR (KBr): 3365, 1656, 1621, 1583, 1418, 1360, 1323, 1290, 1207, 1068, 1045, 900, 796, 746, 665; HRMS-ESI (m/z): calcd for $C_{14}H_{11}ClNaO_3$ [$M + Na$]⁺ 285.0289, found: 285.0290.

4.1.2.6. 2-Hydroxy-7-bromo-3-(2-methylprop-1-enyl)naphthalene-1,4-dione (3f). Yellow solid, m.p. 160–161 °C, yield 61%; ¹H NMR (400 MHz, DMSO- d_6) δ : 11.10 (s, 1H), 8.06–8.00 (m, 2H), 7.86 (d, 1H, $J = 8.0$ Hz), 5.82 (t, 1H, $J = 1.2$ Hz), 1.88 (d, 3H, $J = 1.2$ Hz), 1.55 (d, 3H, $J = 0.8$ Hz); ¹³C NMR (100 MHz, DMSO- d_6) δ : 184.0, 180.5, 154.5, 140.9, 137.4, 132.2, 131.4, 128.5, 128.3, 127.4, 121.3, 115.2, 26.5, 21.9; IR (KBr): 3365, 1623, 1579, 1412, 1359, 1289, 1248, 1206, 1045, 895, 859, 792, 744, 665; HRMS-ESI (m/z): calcd for $C_{14}H_{11}BrNaO_3$ [$M + Na$]⁺ 328.9784, found: 328.9789.

4.1.2.7. *2-Hydroxy-5-methoxy-3-(2-methylprop-1-enyl)naphthalene-1,4-dione (3g)*. Yellow solid, m.p. 122–123 °C; ^1H NMR (400 MHz, DMSO- d_6) δ : 10.51 (s, 1H), 7.72 (t, 1H, $J = 7.6$ Hz), 7.63 (dd, 1H, $J = 0.8$, 7.6 Hz), 7.52 (dd, 1H, $J = 0.8$, 8.4 Hz), 5.82 (t, 1H, $J = 1.6$ Hz), 4.12 (s, 3H), 1.88 (d, 3H, $J = 1.2$ Hz), 1.54 (d, 3H, $J = 0.8$ Hz); ^{13}C NMR (100 MHz, DMSO- d_6) δ : 184.1, 181.8, 159.3, 152.1, 140.2, 134.6, 132.6, 122.6, 120.2, 119.7, 118.6, 115.9, 56.8, 26.6, 21.8; IR (KBr): 3369, 1638, 1582, 1474, 1449, 1382, 1267, 1191, 1064, 1035, 973, 889, 758, 666; HRMS-ESI (m/z): calcd for $\text{C}_{15}\text{H}_{14}\text{NaO}_4$ [$\text{M} + \text{Na}$] $^+$ 281.0784, found: 281.0786.

4.1.2.8. *2-Hydroxy-5,7-dimethyl-3-(2-methylprop-1-enyl)naphthalene-1,4-dione (3h)*. Yellow solid, m.p. 144–145 °C, yield 58%; ^1H NMR (400 MHz, DMSO- d_6) δ : 10.60 (s, 1H), 7.72 (s, 1H), 7.43 (s, 1H), 5.84 (t, 1H, $J = 1.2$ Hz), 2.60 (s, 3H), 2.39 (s, 3H), 1.87 (d, 3H, $J = 1.2$ Hz), 1.54 (d, 3H, $J = 0.8$ Hz); ^{13}C NMR (100 MHz, DMSO- d_6) δ : 187.0, 182.1, 152.7, 142.9, 140.4, 139.3, 131.9, 127.6, 125.4, 122.1, 116.0, 26.5, 22.7, 21.8, 21.3; IR (KBr): 3344, 2976, 2907, 1600, 1435, 1377, 1326, 1293, 1190, 1092, 898, 880, 756, 677; HRMS-ESI (m/z): calcd for $\text{C}_{16}\text{H}_{16}\text{NaO}_3$ [$\text{M} + \text{Na}$] $^+$ 279.0992, found: 279.0992.

4.1.2.9. *2-Hydroxy-6,7-dimethoxy-3-(2-methylprop-1-enyl)naphthalene-1,4-dione (3i)*. Red solid, m.p. 161–162 °C, yield 83%; ^1H NMR (400 MHz, DMSO- d_6) δ : 10.75 (s, 1H), 7.41 (d, 1H, $J = 9.2$ Hz), 5.80 (t, 1H, $J = 1.6$ Hz), 3.93 (s, 3H), 3.92 (s, 3H), 1.87 (d, 3H, $J = 1.2$ Hz), 1.54 (d, 3H, $J = 0.8$ Hz); ^{13}C NMR (100 MHz, DMSO- d_6) δ : 184.3, 180.8, 154.1, 152.7, 140.0, 127.3, 124.5, 120.0, 115.5, 108.3, 107.9, 56.5 (2C), 26.5, 21.8; IR (KBr): 3347, 1633, 1576, 1463, 1302, 1207, 1126, 1038, 978, 885, 751, 637; HRMS-ESI (m/z): calcd for $\text{C}_{16}\text{H}_{16}\text{NaO}_5$ [$\text{M} + \text{Na}$] $^+$ 311.0890, found: 311.0894.

4.1.3. Synthesis of 3-(1-benzotriazole)-nor- β -lapachone 5

Bromine (2 mL) was added to a solution of nor-lapachol 3 (228 mg, 1 mmol) in 25 mL of chloroform. The bromo intermediate precipitated immediately as an orange solid, and the reaction mixture was left under stirring conditions for an additional 10 min. After the removal of excess bromine, a solution of benzotriazoles (1 mmol) in 25 mL of chloroform was added and stirred overnight. The mixture was poured into 50 mL of water. The organic phase was separated and washed with saturated NaHCO_3 solution, dried over Na_2SO_4 , filtered, and evaporated under reduced pressure to yield a solid, which was purified by column chromatography using petroleum ether and ethyl acetate as a eluent.

4.1.3.1. *3-(1H-Benzo[d][1,2,3]triazol-1-yl)-2,3-dihydro-2,2-dimethylnaphtho[1,2-b]furan-4,5-dione (5a)*. Orange solid, m.p. 198–199 °C, yield 58%; ^1H NMR (400 MHz, CDCl_3) δ : 8.21–8.05 (m, 2H), 7.88–7.72 (m, 3H), 7.47–7.38 (m, 3H), 6.25 (s, 1H), 1.84 (s, 3H), 1.13 (s, 3H); ^{13}C NMR (100 MHz, CDCl_3) δ : 180.2, 174.6, 171.0, 146.2, 134.9, 133.2, 133.1, 131.5, 130.0, 128.2, 126.8, 125.5, 124.3, 120.5, 120.2, 109.1, 95.5, 65.6, 28.0, 21.3; IR (KBr): 2925, 1653, 1619, 1491, 1406, 1249, 1218, 1076, 749; HRMS-ESI (m/z): calcd for $\text{C}_{20}\text{H}_{15}\text{N}_3\text{NaO}_3$ [$\text{M} + \text{Na}$] $^+$ 368.1006, found: 368.1006.

4.1.3.2. *3-(1H-Benzo[d][1,2,3]triazol-1-yl)-2,3-dihydro-2,2,7-trimethylnaphtho[1,2-b]furan-4,5-dione (5b)*. Red solid, m.p. 190–191 °C, yield 43%; ^1H NMR (400 MHz, CDCl_3) δ : 8.09–7.92 (m, 2H), 7.74 (d, 1H, $J = 7.6$ Hz), 7.57 (d, 1H, $J = 7.6$ Hz), 7.46–7.37 (m, 3H), 6.23 (s, 1H), 2.52 (s, 3H), 1.82 (s, 3H), 1.12 (s, 3H); ^{13}C NMR (100 MHz, CDCl_3) δ : 180.6, 174.6, 171.3, 146.2, 144.5, 135.3, 131.5, 131.1, 130.8, 128.1, 125.6, 125.3, 124.2, 120.6 (2C), 109.1, 95.3, 65.6, 28.0, 21.8, 21.3; IR (KBr): 2923, 1655, 1608, 1564, 1505, 1417, 1355, 1239, 1161, 1097, 1078, 791, 746, 662; HRMS-ESI (m/z): calcd for $\text{C}_{21}\text{H}_{17}\text{N}_3\text{NaO}_3$ [$\text{M} + \text{Na}$] $^+$ 382.1162, found: 382.1166.

4.1.3.3. *3-(1H-Benzo[d][1,2,3]triazol-1-yl)-2,3-dihydro-7-methoxy-2,2-dimethylnaphtho[1,2-b]furan-4,5-dione (5c)*. Orange solid, m.p. 192–193 °C, yield 69%; ^1H NMR (400 MHz, CDCl_3) δ : 8.07 (d, 1H, $J = 8.4$ Hz), 7.77 (d, 1H, $J = 8.4$ Hz), 7.69 (d, 1H, $J = 2.4$ Hz), 7.44–7.22 (m, 4H), 6.23 (s, 1H), 3.97 (s, 3H), 1.81 (s, 3H), 1.11 (s, 3H); ^{13}C NMR (100 MHz, CDCl_3) δ : 180.4, 174.6, 171.6, 163.9, 146.3, 133.6, 133.0, 128.0, 127.5, 12.67, 124.2, 120.5 (2C), 119.3, 114.9, 109.2, 95.4, 65.7, 56.1, 28.0, 21.3; IR (KBr): 3001, 1656, 1601, 1563, 1448, 1413, 1350, 1278, 1114, 1097, 844, 822, 743; HRMS-ESI (m/z): calcd for $\text{C}_{21}\text{H}_{17}\text{N}_3\text{NaO}_4$ [$\text{M} + \text{Na}$] $^+$ 398.1111, found: 398.1112.

4.1.3.4. *3-(1H-Benzo[d][1,2,3]triazol-1-yl)-2,3-dihydro-7-fluoro-2,2-dimethylnaphtho[1,2-b]furan-4,5-dione (5d)*. Orange solid, m.p. 210–211 °C, yield 70%; ^1H NMR (400 MHz, CDCl_3) δ : 8.08 (d, 1H, $J = 8.4$ Hz), 7.90–7.86 (m, 2H), 7.49–7.36 (m, 4H), 6.20 (s, 1H), 1.82 (s, 3H), 1.12 (s, 3H); ^{13}C NMR (100 MHz, CDCl_3) δ : 179.2, 174.2, 170.2, 165.8 (d, $J_{\text{C-F}} = 250.9$ Hz), 146.2, 134.1 (d, $J_{\text{C-F}} = 8.1$ Hz), 128.1 (d, $J_{\text{C-F}} = 14.2$ Hz), 127.9, 124.3, 123.2, 123.1, 121.7 (d, $J_{\text{C-F}} = 22.4$ Hz), 120.6 (2C), 117.5 (d, $J_{\text{C-F}} = 24$ Hz), 109.0, 95.7, 65.4, 28.0, 21.3; IR (KBr): 3054, 1656, 1617, 1582, 1415, 1267, 1247, 1080, 797, 737; HRMS-ESI (m/z): calcd for $\text{C}_{20}\text{H}_{14}\text{FN}_3\text{NaO}_3$ [$\text{M} + \text{Na}$] $^+$ 386.0911, found: 386.0910.

3-(1H-Benzo[d][1,2,3]triazol-1-yl)-2,3-dihydro-7-chloro-2,2-dimethylnaphtho[1,2-b]furan-4,5-dione (5e). Orange solid, m.p. 204–205 °C, yield 34%; ^1H NMR (400 MHz, CDCl_3) δ : 8.15 (d, 1H, $J = 2.0$ Hz), 8.08 (d, 1H, $J = 8.0$ Hz), 7.81–7.73 (m, 2H), 7.50–7.37 (m, 3H), 6.20 (s, 1H), 1.82 (s, 3H), 1.12 (s, 3H); ^{13}C NMR (100 MHz, CDCl_3) δ : 179.3, 173.9, 170.1, 146.2, 140.3, 134.7, 133.1, 132.7, 130.1, 128.2, 126.8, 125.1, 124.3, 120.6 (2C), 108.9, 95.8, 65.4, 28.0, 21.3; IR (KBr): 3067, 1655, 1615, 1579, 1493, 1398, 1215, 1100, 1082, 865, 747; HRMS-ESI (m/z): calcd for $\text{C}_{20}\text{H}_{14}\text{ClN}_3\text{NaO}_3$ [$\text{M} + \text{Na}$] $^+$ 402.0616, found: 402.0614.

4.1.3.5. *3-(1H-Benzo[d][1,2,3]triazol-1-yl)-2,3-dihydro-7-bromo-2,2-dimethylnaphtho[1,2-b]furan-4,5-dione (5f)*. Orange solid, m.p. 205–206 °C, yield 55%; ^1H NMR (400 MHz, CDCl_3) δ : 8.29 (d, 1H, $J = 2.0$ Hz), 8.07 (d, 1H, $J = 8.4$ Hz), 7.91 (dd, 1H, $J = 2.0$, 8.0 Hz), 7.71 (d, 1H, $J = 8.0$ Hz), 7.47–7.36 (m, 3H), 6.20 (s, 1H), 1.82 (s, 3H), 1.13 (s, 3H); ^{13}C NMR (100 MHz, CDCl_3) δ : 179.2, 173.8, 170.2, 146.2, 137.7, 133.5, 133.1, 132.5, 128.6, 128.2, 126.8, 125.5, 124.3, 120.6 (2C), 108.9, 95.8, 65.4, 28.0, 21.3; IR (KBr): 1653, 1613, 1579, 1486, 1397, 1230, 1094, 1075, 1009, 739; HRMS-ESI (m/z): calcd for $\text{C}_{20}\text{H}_{14}\text{BrN}_3\text{NaO}_3$ [$\text{M} + \text{Na}$] $^+$ 446.0111, found: 446.0114.

4.1.3.6. *3-(1H-Benzo[d][1,2,3]triazol-1-yl)-2,3-dihydro-9-methoxy-2,2-dimethylnaphtho[1,2-b]furan-4,5-dione (5g)*. Red solid, m.p. 254–255 °C, yield 52%; ^1H NMR (400 MHz, CDCl_3) δ : 8.07 (d, 1H, $J = 8.4$ Hz), 7.84 (dd, 1H, $J = 0.8$, 7.2 Hz), 7.66 (t, 1H, $J = 8.0$ Hz), 7.45 (d, 1H, $J = 3.2$ Hz), 7.38–7.32 (m, 2H), 6.18 (s, 1H), 4.01 (s, 3H), 1.80 (s, 3H), 1.12 (s, 3H); ^{13}C NMR (100 MHz, CDCl_3) δ : 180.7, 174.4, 172.2, 158.5, 146.2, 134.5, 133.4, 133.1, 128.0, 124.1, 123.3, 120.5 (2C), 119.2, 114.2, 109.3, 94.7, 64.8, 56.7, 28.1, 21.3; IR (KBr): 1698, 1648, 1595, 1480, 1355, 1279, 1109, 1067, 750; HRMS-ESI (m/z): calcd for $\text{C}_{21}\text{H}_{17}\text{N}_3\text{NaO}_4$ [$\text{M} + \text{Na}$] $^+$ 398.1111, found: 398.1114.

4.1.3.7. *3-(1H-Benzo[d][1,2,3]triazol-1-yl)-2,3-dihydro-2,2,7,9-tetramethylnaphtho[1,2-b]furan-4,5-dione (5h)*. Red solid, m.p. 197–198 °C, yield 41%; ^1H NMR (400 MHz, CDCl_3) δ : 8.06 (d, 1H, $J = 8.0$ Hz), 7.91 (s, 1H), 7.44–7.35 (m, 4H), 6.20 (s, 1H), 2.69 (s, 3H), 2.45 (s, 3H), 1.81 (s, 3H), 1.12 (s, 3H); ^{13}C NMR (100 MHz, CDCl_3) δ : 180.0, 174.7, 173.6, 146.2, 143.8, 139.4, 139.2, 133.1, 132.8, 129.8, 128.1, 124.2, 122.1, 120.5 (2C), 109.2, 94.8, 64.9, 28.2, 22.1, 21.5, 21.4; IR (KBr): 2922, 1649, 1608, 1585, 1450, 1343, 1282, 1246, 1103, 1075, 778, 746; HRMS-ESI (m/z): calcd for $\text{C}_{22}\text{H}_{19}\text{N}_3\text{NaO}_3$ [$\text{M} + \text{Na}$] $^+$ 396.1319, found: 396.1318.

4.1.3.8. *3-(1H-Benzo[d][1,2,3]triazol-1-yl)-2,3-dihydro-7,8-dimethoxy-2,2-dimethylnaphtho[1,2-b]furan-4,5-dione (5i)*. Red solid, m.p. 212–214 °C, yield 63%; ¹H NMR (400 MHz, CDCl₃) δ: 8.06 (d, 1H, *J* = 8.4 Hz, H-4'), 7.65 (s, 1H, H-6), 7.43–7.34 (m, 3H, H-5', 6', 7'), 7.25 (s, 1H, H-9), 6.23 (s, 1H, H-3), 4.08 (s, 3H, 7-OCH₃), 4.02 (s, 3H, 7-OCH₃), 1.81 (s, 3H, 2-CH₃), 1.11 (s, 3H, 2-CH₃); ¹³C NMR (100 MHz, CDCl₃) δ: 179.3 (C-5), 174.9 (C-4), 171.1 (C-9b), 154.2 (C-8), 152.7 (C-7), 146.2 (C-3'a), 133.0 (7'a), 128.1 (C-6'), 126.0 (C-9a), 124.2 (C-5'), 121.2 (C-5a), 120.4 (C-4'), 112.3 (C-6), 109.4 (C-3a), 109.3 (C-7'), 107.4 (C-9), 95.5 (C-2), 65.8 (C-3), 56.7 (C-7), 56.6 (C-8), 28.0 (2-CH₃), 21.3 (2-CH₃); IR (KBr): 2919, 1654, 1612, 1572, 1516, 1396, 1355, 1280, 1222, 1134, 1022, 779, 747; HRMS-ESI (*m/z*): calcd for C₂₂H₁₉N₃NaO₅ [M + Na]⁺ 428.1217, found: 428.1214.

4.1.3.9. *3-(5-Methyl-1H-benzo[d][1,2,3]triazol-1-yl)-2,3-dihydro-2,2-dimethylnaphtho[1,2-b]furan-4,5-dione (5j)*. Red solid, m.p. 224–225 °C, yield 68%; ¹H NMR (400 MHz, CDCl₃) δ: 8.18 (d, 1H, *J* = 7.6 Hz), 7.94–7.71 (m, 4H), 7.32–7.11 (m, 3H), 6.20 (s, 1H), 2.49 (s, 3H), 1.82 (s, 3H), 1.12 (s, 3H); ¹³C NMR (100 MHz, CDCl₃) δ: 180.2, 174.6, 170.9, 144.8, 138.8, 134.8, 134.3, 133.2, 131.6, 130.2, 130.0, 128.1, 126.5, 125.5 (2C), 124.1, 119.9, 108.6, 95.5, 65.6, 28.0, 21.3, 16.8; IR (KBr): 2982, 1651, 1615, 1570, 1493, 1412, 1353, 1223, 1115, 1083, 800, 762, 726; HRMS-ESI (*m/z*): calcd for C₂₁H₁₇N₃NaO₃ [M + Na]⁺ 382.1162, found: 382.1164.

4.1.3.10. *3-(5-Butyl-1H-benzo[d][1,2,3]triazol-1-yl)-2,3-dihydro-2,2-dimethylnaphtho[1,2-b]furan-4,5-dione (5k)*. Yellow solid, m.p. 113–114 °C, yield 41%; ¹H NMR (400 MHz, CDCl₃) δ: 8.17 (dd, 1H, *J* = 1.2, 7.6 Hz), 7.95–7.70 (m, 4H), 7.29–7.19 (m, 2H), 6.21 (s, 1H), 2.74 (t, 2H, *J* = 7.6 Hz), 1.81 (s, 3H), 1.66–1.60 (m, 2H), 1.39–1.26 (m, 2H), 1.12 (s, 3H), 0.95–0.84 (m, 3H); ¹³C NMR (100 MHz, CDCl₃) δ: 180.3, 174.6, 170.9, 146.8, 143.7, 139.4, 134.9, 133.2, 131.5, 129.9, 129.7, 126.8, 125.9, 125.5, 119.9, 118.8, 108.7, 95.5, 65.6, 35.4, 33.6, 28.0, 22.0, 21.3, 13.9; IR (KBr): 2931, 1658, 1619, 1589, 1572, 1493, 1408, 1220, 1083, 775; HRMS-ESI (*m/z*): calcd for C₂₄H₂₃N₃NaO₃ [M + Na]⁺ 424.1632, found: 424.1634.

4.1.3.11. *3-(5-Chloro-1H-benzo[d][1,2,3]triazol-1-yl)-2,3-dihydro-2,2-dimethylnaphtho[1,2-b]furan-4,5-dione (5l)*. Orange solid, m.p. 255–257 °C, yield 67%; ¹H NMR (400 MHz, CDCl₃) δ: 8.06 (s, 1H), 7.86 (d, 1H, *J* = 6.8 Hz), 7.81–7.74 (m, 3H), 7.41–7.34 (m, 2H), 6.18 (s, 1H), 1.83 (s, 3H), 1.13 (s, 3H); ¹³C NMR (100 MHz, CDCl₃) δ: 180.1, 174.6, 171.0, 146.8, 134.9, 133.4, 131.8, 131.6, 130.2, 130.1, 129.1, 126.7, 125.6 (2C), 119.9, 110.0, 65.9, 95.4, 28.1, 21.3; IR (KBr): 1654, 1616, 1587, 1570, 1493, 1412, 1351, 1256, 1221, 1113, 1081, 1055, 778; HRMS-ESI (*m/z*): calcd for C₂₀H₁₄ClN₃NaO₃ [M + Na]⁺ 402.0616, found: 402.0617.

4.1.4. Synthesis of 3-(4-aryl-1,2,3-triazol)-nor-β-lap 8

To a mixture of 3-azido-2,2-dimethyl-2,3-dihydro-naphtho[1,2-b]furan-4,5-dione **6** (135 mg, 0.5 mmol), CuSO₄ (4 mg, 0.025 mmol) and sodium ascorbate (20 mg, 0.1 mmol) in 12 mL *t*-BuOH/H₂O (1:1 v/v), the corresponding alkyne **7** (0.55 mmol) was added. The mixture was stirred overnight at room temperature. The organic phase was extracted with dichloromethane, dried with NaSO₄ and concentrated under reduced pressure. The residue obtained was purified by column chromatography on silica gel using a gradient mixture of CH₂Cl₂/ethyl acetate as eluent with increasing polarity.

4.1.4.1. *2,2-Dimethyl-3-(4-phenyl-[1,2,3]triazol-1-yl)-2,3-dihydro-naphtho[1,2-b]furan-4,5-dione (8a)*. Yellow solid, m.p. 144–145 °C, yield 91%; ¹H NMR (400 MHz, CDCl₃) δ: 8.20 (dd, 1H, *J* = 1.2, 7.2 Hz), 7.84–7.73 (m, 6H), 7.40–7.31 (m, 3H), 6.03 (s, 1H), 1.79 (s, 3H), 1.25 (s, 3H); ¹³C NMR (100 MHz, CDCl₃) δ: 180.1, 174.5, 171.3, 147.6, 134.9, 133.4, 131.5, 130.1, 130.0, 128.8 (2C), 128.3, 126.6, 125.8 (2C), 125.6,

119.0, 111.2, 96.1, 66.9, 21.7, 21.2; HRMS-ESI (*m/z*): calcd for C₂₂H₁₇N₃NaO₃ [M + Na]⁺ 394.1162, found: 394.1160.

4.1.4.2. *2,2-Dimethyl-3-(4-*p*-tolylphenyl)-[1,2,3]triazol-1-yl)-2,3-dihydro-naphtho[1,2-b]furan-4,5-dione (8b)*. Yellow solid, m.p. 154–155 °C, yield 93%; ¹H NMR (400 MHz, CDCl₃) δ: 8.18 (dd, 1H, *J* = 1.2, 7.2 Hz), 7.83–7.66 (m, 6H), 7.18 (d, 2H, *J* = 8.0 Hz), 6.01 (s, 1H), 2.35 (s, 3H), 1.77 (s, 3H), 1.24 (s, 3H); ¹³C NMR (100 MHz, CDCl₃) δ: 180.1, 174.5, 171.3, 147.7, 138.1, 134.9, 133.4, 131.5, 130.0, 129.4 (2C), 127.3, 126.7, 125.6 (2C), 118.7, 111.3, 96.1, 66.8, 27.7, 21.3, 21.2; HRMS-ESI (*m/z*): calcd for C₂₃H₁₉N₃NaO₃ [M + Na]⁺ 408.1319, found: 408.1316.

4.1.4.3. *2,2-Dimethyl-3-(4-*p*-butylphenyl)-[1,2,3]triazol-1-yl)-2,3-dihydro-naphtho[1,2-b]furan-4,5-dione*. Yellow solid, m.p. 160–161 °C, yield 89%; ¹H NMR (400 MHz, CDCl₃) δ: 8.19 (dd, 1H, *J* = 1.2, 7.2 Hz), 7.83–7.69 (m, 6H), 7.19 (d, 2H, *J* = 8.0 Hz), 6.02 (s, 1H), 2.60 (t, 2H, *J* = 8.0 Hz), 1.77 (s, 3H), 1.64–1.55 (m, 2H), 1.37–1.26 (m, 2H), 1.24 (s, 3H), 0.91 (s, 3H); ¹³C NMR (100 MHz, CDCl₃) δ: 180.1, 174.5, 171.3, 147.7, 143.3, 134.9, 133.4, 131.5, 130.0, 128.8 (2C), 127.4, 126.7, 125.7 (2C), 125.6, 118.7, 111.3, 96.1, 66.9, 35.4, 33.5, 27.7, 22.3, 21.2, 13.9; HRMS-ESI (*m/z*): calcd for C₂₆H₂₅N₃NaO₃ [M + Na]⁺ 450.1785, found: 450.1788.

4.1.5. Synthesis of nor-β-lap

Nor-β-lap was prepared by cyclization of **3a** in the presence of H₂SO₄ according to the reported method [35]. A mixture of quinone **3a** (228 mg, 1 mmol) in sulfuric acid (5 mL) was stirred for 30 min at 25 °C. The solution was then poured into 60 mL of cold water and extracted with ethyl acetate. After removal of the solvent, the product was recrystallized by EtOH to give nor-β-lap as an orange solid, 220 mg, yield 96%, m.p. 169–170 °C. ¹H NMR (400 MHz, CDCl₃) δ: 8.08 (d, 1H, *J* = 7.2 Hz), 7.66–7.56 (m, 3H), 2.96 (s, 2H), 1.61 (s, 3H); ¹³C NMR (100 MHz, CDCl₃) δ: 181.3, 175.7, 168.7, 134.4, 131.9, 130.9, 129.3, 128.0, 124.6, 115.0, 93.7, 39.3, 28.4 (2C); IR (KBr): 2977, 1692, 1641, 1608, 1585, 1564, 1491, 1444, 1410, 1355, 1273, 1211, 1114, 1080, 972, 901, 839, 771, 723, 690, 662, 535, 437; HRMS-ESI (*m/z*): calcd for C₁₄H₁₂NaO₃ [M + Na]⁺ 251.0679, found: 251.0678.

4.2. Enzyme reduction assay in vitro

The human recombinant NQO1 (Sigma) as well as NADPH recycling test was carried out to determine the NQO1-induced compound metabolic rates, where the oxidation of NADPH into NADP⁺ was determined using the UV-Visible Spectrophotometer (UV-2550, Shimadzu, Japan) based on NADPH oxidation amount at A_{340nm}. Thereafter, a 10 μL of the test compound contained in DMSO stock was added to a 0.2 mm cuvette, followed by the addition of 490 μL NADPH (400 mmol/L) together with NQO1 (1.4 mg/mL) contained in the phosphate buffer (50 mmol/L, pH 7.4). After transferring the cuvette into an instrument filled with assay solution in addition to the NADPH solution. Then, the enzymatic reaction was initiated through the automatic dispersion of NADPH solution into the cuvette, and each value was determined once at the intervals of 5 s for 1 min at room temperature. The linearity graphs on the absorbance as a function of time (between the first 20 s and 1 min) were fitted, and the velocity values were determined as well. Besides, the initial velocity values were calculated, and all data were expressed as μmol oxidized NADPH per μmol protein per minute.

4.3. Molecular modeling

Molecular docking study was carried out for determining the binding pattern of compound with NQO1 by the use of Autodock vina 1.1.2 software. For human NQO1 (PDB ID: 2F1O), its 3D structure was obtained based on the protein data bank (<http://www.rcsb.org/pdb/home/home.do>). The chembio3D ultra 14.0 and chembiodraw ultra 14.0

were utilized to draw the compound's 3D structure. The docking input files were generated by autodock tools 1.5.6 package. For NQO1, its search grid was recognized to be center_x: 11.549, center_y: 11.875, and center_z: -6.018, and the dimensions were size_x: 15, size_y: 15 and size_z: 15. Meanwhile, the exhaustiveness value was 20. To carry out vina docking, each default parameter was adopted unless specified otherwise. The PyMol1.7.6 (<http://www.pymol.org/>) was utilized for the selection and visual analysis of the optimal-scoring pose determined through vina docking score. By re-docking the original ligand DIC with these settings, its co-crystallized conformation was reproduced approximately (RMSD: 0.51 Å), which indicates the validity of the protocol used.

4.4. Cell growth inhibitory activity

The MTT assay was conducted to determine compound cytotoxicity. The MCF-7 and A549 cells were inoculated into the high-glucose DMEM, whereas the HepG2 and LO2 cells were inoculated in the RPMI1640 containing 10% FBS. Then, the cells were subjected to 24 h incubation under 37 °C and CO₂ conditions, followed by 48 h of compound treatment. Afterwards, 10 µL MTT was put into all wells, followed by another 4 h of incubation. After removing supernatant from all wells, the formazan crystal was sufficiently mixed with 150 µL DMSO, and the absorbance was determined at 568 nm.

4.5. Analysis of cell cycle

Flow cytometry was conducted for evaluating cell cycle distribution. To this end, the HepG2 cells were subjected to 24 h of **5k** treatments at 0.5, 1.0, 2.0 µM. Then, the untreated as well as the treated cells were collected; after washing by PBS, the cells were fixed within the ice-cold 70% ethanol, followed by PI staining. Then, flow cytometry was performed to analyze the cell cycle distribution.

4.6. Apoptosis assays

Cell apoptosis was measured through Annexin-V/PI staining. The HepG2 cells were treated by **5k** (1.2, 2.4, 4.8 µM) for 24 h. Thereafter, Annexin-V conjugated by fluorescein isothiocyanate (FITC) was adopted for detecting the apoptotic cells, whereas PI was applied in detecting the necrotic cells. Then, the overall cell death was determined by combining apoptotic cell number with necrotic cell count. The apoptosis test was carried out in accordance with specific protocols. In brief, after the 1×10^7 treated cells were washed by PBS, cells were resuspended into the Annexin-V/PI staining solution, followed by immediate analysis by flow cytometry. Each assay was carried out for three replicates.

4.7. MMP measurements

MMP was determined using the lipophilic cationic dye JC-1 (Molecular Probes). Compound **5k** was used to treat the cultures for 48 h at 1.2, 2.4 and 4.8 µM. Then, the HepG2 cells were subjected to 20 min of JC-1 incubation under 37 °C. After that, the incubated cultures were used to measure MMP in accordance with specific protocols, and the flow cytometry was performed to measure any shift in MMP.

4.8. Intracellular ROS level determination

The intracellular ROS generation was measured via the peroxide-sensitive fluorescence probe DCF-DA. Briefly, a 5 µM of **5k** was used to treat HepG2 cells for 3 and 5 h, followed by 15 min of incubation using 10 µM DCF-DA under 37 °C. DCF-DA oxidation into 2',7'-dichlorofluorescein (DCF, the fluorescence compound) was regulated by intracellular ROS. Thereafter, all cells were collected, and then 1 mL PBS was used to suspend cell pellets. Each sample was determined at the excitation and emission wave lengths of 480 nm and 525 nm,

respectively, through the FACS Calibur flow cytometry.

4.9. Electrochemical studies

Cyclic voltammetry (CV) for representative compounds was conducted using CHI 660A electrochemical workstation equipped with a conventional three-electrode system, in which the modified glassy carbon electrode (GCE) was the working electrode, a platinum wire was the counter electrode and an Ag/AgCl (sat. KCl) was the reference electrode. The reference electrode was separated from the main compartment of the system by a salt bridge containing DMF solvent and Bu₄NBF₄ supporting electrolyte. The reference and the salt bridge were calibrated by voltammetry relative to Eredox for Ferrocene (0/+) couple in DMF/Bu₄NBF₄, to allow the measured Eredox values for the compounds to be quoted relative to Ferrocene (0/+). All of the compounds were run at concentration of 1 mM in DMF and all samples were purged with nitrogen prior to use and kept under a continuous flow of nitrogen during the course of the experiments. All data were recorded at a potential range between 0.00 and -2.00 V and at potential sweep rates of 50 mV/s.

4.10. TBARS assays

The lipid peroxidation was determined by the reaction of thiobarbituric acid (TBA) with malondialdehyde (MDA). HepG2 Cells were incubated with **5k** (5 and 10 µM) and nor-β-lap (5 and 10 µM) for 24 h and then lysed with 15 mM Tris-HCl for 1 h. Two mL of trichloroacetic acid (0.4 mg/mL) and HCl (0.25 M) was added to the lysate, which was then incubated with 7 mg/mL TBA for 15 min at 100 °C. The mixture was centrifuged at 900 g for 15 min. Results are expressed in terms of thiobarbituric reactive species (TBARS), which are determined by absorbance at 532 nm. The results were normalized by protein content.

4.11. Antitumor effect in vivo

Compound **5k** or β-lap was dissolved in 5% DMSO, 2% poloxamer as well as 93% saline. Thereafter, the HepG2 cells were inoculated. Then, 0.2 mL cell suspension was injected into the flanks of athymic nude mice with 7–8 weeks old. When the tumor grew to 60–80 mm³, all animals were randomized into three groups (n = 5), namely, vehicle (saline), β-lap (20 mg/kg) or **5k** (20 mg/kg) group. Animals in vehicle and drug groups were given corresponding treatment through the tail vein every two days for altogether 19 days, and the tumor growth was determined once a day. Tumor size was determined at regular period by the use of calipers, whereas tumor volume was measured according to the formula of volume (mm³) = length × width × width/2. At the end of the experiments, each animal was sacrificed for tumor dissection and weighing following the guidance of the Animal Care and Welfare Committee of Shandong University and the principles outlined in the Declaration of Helsinki for animal experimental investigations. The effect of **5k** on tumor growth was expressed as percentage compared with vehicle group.

Declaration of Competing Interest

The authors declare that they have no known competing financial interests or personal relationships that could have appeared to influence the work reported in this paper.

Acknowledgements

This work is financially supported by NSFC-Henan Joint Fund (No. U1604164).

Appendix A. Supplementary material

Supplementary data to this article can be found online at <https://doi.org/10.1016/j.bioorg.2021.104995>.

References

- [1] F. Bray, J. Ferlay, I. Soerjomataram, R.L. Siegel, L.A. Torre, A. Jemal, Global cancer statistics, *GLOBOCAN estimates of incidence and mortality worldwide for 36 cancers in 185 countries*, *CA Cancer J. Clin.* 68 (2018) 394–424.
- [2] B.D. Kurmi, P. Patel, R. Paliwal, S.R. Paliwal, Molecular approaches for targeted drug delivery towards cancer: A concise review with respect to nanotechnology, *J. Drug Del. Sci. Tec.* 57 (2020), 101682.
- [3] A. Buzdin, M. Sorokin, A. Garazha, M. Sekacheva, E. Kim, N. Zhukov, Y. Wang, X. M. Li, S. Kar, C. Hartmann, A. Samii, A. Giese, N. Borisov, Molecular pathway activation-New type of biomarkers for tumor morphology and personalized selection of target drugs, *Semi. Cancer Biol.* 53 (2018) 110–124.
- [4] R. Li, Q. Li, Q. Ji, Molecular targeted study in tumors: From western medicine to active ingredients of traditional Chinese medicine, *Biomed. Pharmacother.* 121 (2020), 109624.
- [5] M. Dobbstein, U. Moll, Targeting tumour-supportive cellular machineries in anticancer drug development, *Nat. Rev. Drug Discov.* 13 (2014) 179–196.
- [6] D. Siegel, D.L. Gustafson, D.L. Dehn, J.Y. Han, Preecha Boonchoong, Lawrence J. Berliner, David Ross, NAD(P)H: quinone oxidoreductase 1: role as a superoxide scavenger, *Mol. Pharmacol.* 65 (2004) 1238–1247.
- [7] S. Danson, T.H. Ward, J. Butler, M. Ranson, DT-diaphorase: a target for new anticancer drugs, *Cancer Treat. Rev.* 30 (2004) 437–449.
- [8] F.J. Alcaín, J.M. Villalba, NQO1-directed antitumour quinones, *Expert Opin. Ther. Pat.* 17 (2007) 649–665.
- [9] K. Zhang, D. Chen, K. Ma, X. Wu, H. Hao, S. Jiang, NAD(P)H: Quinone oxidoreductase 1 (NQO1) as a therapeutic and diagnostic target in cancer, *J. Med. Chem.* 61 (2018) 6983–7003.
- [10] E.I. Parkinson, J.S. Bair, M. Cismesia, P.J. Hergenrother, Efficient NQO1 substrates are potent and selective anticancer agents, *ACS Chem. Biol.* 8 (2013) 2173–2183.
- [11] M.A. Colucci, C.J. Moody, G.D. Couch, Natural and synthetic quinones and their reduction by the quinone reductase enzyme NQO1: from synthetic organic chemistry to compounds with anticancer potential, *Org. Biomol. Chem.* 6 (2008) 637–656.
- [12] V.F. Ferreira, C.D. Nicoletti, P.G. Ferreira, D.O. Futuro, F.C. da Silva, Strategies for increasing the solubility and bioavailability of anticancer compounds: β -Lapachone and other naphthoquinones, *Curr. Pharmaceut. Des.* 22 (2016) 5899–5914.
- [13] D.R. da Rocha, A.C.G. de Souza, J.A.L.C. Resende, W.C. Santos, E.A. dos Santos, C. Pessoa, M.O. de Moraes, L.V. Costa-Lotufo, R.C. Montenegro, V.F. Ferreira, Synthesis of new 9-hydroxy- α - and 7-hydroxy- β -pyran naphthoquinones and cytotoxicity against cancer cell lines, *Org. Biomol. Chem.* 9 (2011) 4315–4322.
- [14] E.N. da Silva Júnior, C.F. de Deus, B.C. Cavalcanti, C. Pessoa, L.V. Costa-Lotufo, R. C. Montenegro, M.O. de Moraes, M.C.F.R. Pinto, C.A. de Simone, V.F. Ferreira, M. O.F. Goulart, C.K.Z. Andrade, A.V. Pinto, 3-Arylamino and 3-alkoxy-*nor*- β -lapachone derivatives: synthesis and cytotoxicity against cancer cell lines, *J. Med. Chem.* 53 (2010) 504–508.
- [15] S.B.B.B. Bahia, W.J. Reis, G.A.M. Jardim, F.T. Souto, C.A. de Simone, C.C. Gatto, R. F.S. Menna-Barreto, S.L. de Castro, B.C. Cavalcanti, C. Pessoa, M.H. Araujo, E.N. da Silva Júnior, Molecular hybridization as a powerful tool towards multitarget quinoidal systems: synthesis, trypanocidal and antitumor activities of naphthoquinone-based 5-iodo-1,4-disubstituted-, 1,4- and 1,5- disubstituted-1,2,3-triazoles, *Med. Chem. Commun.* 7 (2016) 1555–1563.
- [16] E.H.G. da Cruz, M.A. Silvers, G.A.M. Jardim, J.M. Resende, B.C. Cavalcanti, I. S. Bomfim, C. Pessoa, C.A. de Simone, G.V. Botteselle, A.L. Braga, D.K. Nair, I.N. N. Namboothiri, D.A. Boothman, E.N. da Silva Júnior, Synthesis and antitumor activity of selenium-containing quinone-based triazoles possessing two redox centres, and their mechanistic insights, *Eur. J. Med. Chem.* 122 (2016) 1–16.
- [17] S.M. Lim, Y. Jeong, S. Lee, H. Im, H.S. Tae, B.G. Kim, H.D. Park, J. Park, S. Hong, Identification of β -lapachone analogs as novel MALTI inhibitors to treat an aggressive subtype of diffuse large B-cell lymphoma, *J. Med. Chem.* 58 (2015) 8491–8502.
- [18] E.L. Bonifazi, C. Ríos Luci, L.G. León, G. Burton, J.M. Padrón, R.I. Misico, Antiproliferative activity of synthetic naphthoquinones related to lapachol. First synthesis of 5-hydroxylapachol, *Bioorg. Med. Chem.* 18 (2010) 2621–2630.
- [19] E. Pérez-Sacau, R.G. Díaz-Peñate, A. Estévez-Braun, A.G. Ravelo, J.M. García-Castellano, L. Pardo, M. Campillo, Synthesis and pharmacophore modeling of naphthoquinone derivatives with cytotoxic activity in human promyelocytic leukemia HL-60 cell line, *J. Med. Chem.* 50 (2007) 696–706.
- [20] N. Kongkathip, B. Kongkathip, P. Siripong, C. Sangma, S. Luangkamin, M. Niyomdech, S. Pattanapa, S. Piyaviriyagul, P. Kongsaree, Potent antitumor activity of synthetic 1,2-naphthoquinones and 1,4-naphthoquinones, *Bioorg. Med. Chem.* 11 (2003) 3179–3191.
- [21] B.C. Cavalcanti, F.W.A. Barros, I.O. Cabral, J.R.O. Ferreira, H.I.F. Magalhães, H.V. N. Júnior, E.N.S. Júnior, F.C. de Abreu, C.O. Costa, M.O.F. Goulart, M.O. Moraes, C. Pessoa, Preclinical genotoxicology of *nor*- β -lapachone in human cultured lymphocytes and chinese hamster lung fibroblasts, *Chem. Res. Toxicol.* 24 (2011) 1560–1574.
- [22] M.F.D. Cardoso, K. Salomao, A.C. Bombaca, D.R. da Rocha, F.D. da Silva, J.A. S. Cavaleiro, S.L. de Castro, V.F. Ferreira, Synthesis and anti-Trypanosoma cruzi activity of synthetic 1,2-naphthoquinones and 1,4-naphthoquinones, *Bioorg. Med. Chem.* 23 (2015) 4763–4768.
- [23] G.A.M. Jardim, T.T. Guimarães, M.C.F.R. Pinto, B.C. Cavalcanti, K.M. de Farias, C. Pessoa, D.K. Nair, I.N.N. Namboothiri, E.N. da Silva Júnior, Naphthoquinone-based chalcone hybrids and derivatives: synthesis and potent activity against cancer cell lines, *MedChemComm* 6 (2015) 20–130.
- [24] E.N. da Silva Júnior, M.A.B.F. de Moura, A.V. Pinto, M.C.F.R. Pinto, M.C.B.V. de Souza, A.J. Araújo, C. Pessoa, L.V. Costa-Lotufo, R.C. Montenegro, M.O. de Moraes, V.F. Ferreira, M.O.F. Goulart, Cytotoxic, trypanocidal activities and physicochemical parameters of *nor*- β -lapachone-based 1,2,3-triazoles, *J. Braz. Chem. Soc.* 20 (2009) 635–643.
- [25] E.H.G. da Cruz, P.H.P.R. Carvalho, J.R. Correa, D.A.C. Silva, E.B.T. Diogo, J.D. de Souza Filho, B.C. Cavalcanti, C. Pessoa, H.C.B. de Oliveira, B.C. Guido, D.A. da Silva Filho, B.A.D. Neto, E.N. da Silva Júnior, Design, synthesis and application of fluorescent 2,1,3-benzothiadiazole-triazole-linked biologically active lapachone derivatives, *New J. Chem.* 38 (2014) 2569–2580.
- [26] J. Bian, L. Xu, B. Deng, X. Qian, J. Fan, X. Yang, F. Liu, X. Xu, X. Guo, X. Li, H. Sun, Q. You, X. Zhang, Synthesis and evaluation of (\pm)-dunnione and its ortho-quinone analogues as substrates for NAD(P)H:quinone oxidoreductase 1 (NQO1), *Bioorg. Med. Chem. Lett.* 25 (2015) 1244–1248.
- [27] M.F.C. Cardoso, P.C. Rodrigues, M.E.I.M. Oliveira, I.L. Gama, I.M.C.B. da Silva, I. O. Santos, D.R. Rocha, R.T. Pinho, V.F. Ferreira, M.C.B.V. de Souza, F.C. da Silva, F. P. Silva-Jr, Synthesis and evaluation of the cytotoxic activity of 1,2-furanonaphthoquinones tethered to 1,2,3-1H-triazoles in myeloid and lymphoid leukemia cell lines, *E. J. Med. Chem.* 84 (2014) 708–717.
- [28] K. Bajaj, R. Sakhujia, Benzotriazole: Much more than just synthetic heterocyclic chemistry, *Top. Heterocycl. Chem.* 43 (2016) 235–284.
- [29] K.A. Nolan, R. Jer, M.S. Doncaster, K.A. Dunstan, A.D. Scott, D. Frenkel, D. Siegel, D. Ross, J. Barnes, C. Levy, D. Leys, R.C. Whitehead, L.J. Stratford, R.A. Bryce, Synthesis and biological evaluation of coumarin-based inhibitors of NAD(P)H: Quinone oxidoreductase-1 (NQO1), *J. Med. Chem.* 52 (2009) 7142–7156.
- [30] M. Halasi, M. Wang, T.S. Chavan, V. Gaponenko, N. Hay, A.L. Gartel, M. Halasi, et al., ROS inhibitor N-acetyl-L-cysteine antagonizes the activity of proteasome inhibitors, *Biochem. J.* 454 (2013) 201–208.
- [31] B. Deng, S. Xie, J. Wang, Z. Xia, R. Nie, Inhibition of protein kinase C β prevents tumor necrosis factor- α -induced apoptosis and oxidative stress in endothelial cells: The role of NADPH oxidase subunits, *J. Vasc. Res.* 49 (2012) 144–159.
- [32] L. Wu, X. Ma, X. Yang, C. Zhang, Synthesis and biological evaluation of β -lapachone-monastrol hybrids as potential anticancer agents, *Eur. J. Med. Chem.* 203 (2020), 112594.
- [33] S.C. Hooker, Constitution of lapachol and its derivatives. IV. Oxidation with potassium permanganate, *J. Am. Chem. Soc.* 58 (1936) 1168–1173.
- [34] D.R. da Rocha, K. Mota, I.M.C.B. da Silva, V.F. Ferreira, S.B. Ferreira, F.D.C. da Silva, Synthesis of fused chromene-1,4-naphthoquinones via ring-closing metathesis and Knoevenagel-electrocyclization under acid catalysis and microwave irradiation, *Tetrahedron* 70 (2014) 3266–3270.
- [35] W.J. Reis, I.A.O. Bozzi, M.F. Ribeiro, P.C.B. Halicki, L.A. Ferreira, P.E. Almeida da Silva, D.F. Ramos, C.A. de Simone, E.N.J. da Silva, Design of hybrid molecules as antimycobacterial compounds: Synthesis of isoniazid-naphthoquinone derivatives and their activity against susceptible and resistant strains of *Mycobacterium tuberculosis*, *Bioorg. Med. Chem.* 27 (2019) 4143–4150.